Distributed Parallel Algorithm for Finite Element Multi-Computer System Considering Network Security Performance Evaluation

Yi Li

(Corresponding author: Yi Li)

Department of Information Technology, Henan Judicial Police Vocational College
Zhengzhou, Henan 450046, China
Email: jiuersedi@outlook.com

(Received Dec. 20, 2023; Revised and Accepted May 9, 2024; First Online June 22, 2024)

The Special Issue on Cybersecurity and Privacy in the Industrial Internet of Things (IIoT)

Guest Editor: Prof. Zhengyi Chai (Tiangong University, China)

Abstract

In the complex network topology of traditional finite element multi-microcomputer systems, the data transmission process can cause a series of errors. In order to improve the operation effect of finite element multi-computer systems, this paper proposes a distributed parallel algorithm for finite element multi-computer systems considering network security performance evaluation. Taking advantage of the complementarity of DE (Differential Evolution) and EP (Evolutionary Programming), this paper introduces EP under the framework of DE. It constructs a hybrid algorithm named DEEP (Differential Evolution Evolutionary Programming), which is dominated by DE and supplemented by EP. Moreover, this paper adopts the partition clustering technique to obtain a more accurate partition scheme. To verify the correctness of the distributed parallel algorithm, the distributed parallel algorithm proposed in this paper is studied through experiments. This article studies the use of parallel computing technology to accelerate the computational speed of DE for solving reactive power optimization problems and implements it on a microcomputer cluster platform. The required population size is reduced by improving the algorithm itself, thereby further accelerating computation or using smaller clusters to reduce costs. The distributed parallel algorithm proposed in this paper has been verified to have good stability at various frequencies through square wave experiments; the experimental analysis shows that the distributed parallel algorithm proposed in this paper is effective, and it verifies that the distributed parallel algorithm proposed in this paper has a certain promotion effect on the security improvement of the finite element multi-computer system.

Keywords: Finite Element; Multi-computer System; Network Security; Parallel Algorithm

1 Introduction

The microcomputer monitoring system is an important component of the modernization of railway equipment. It integrates the latest modern technologies, such as sensors, fieldbus, computer network communication, databases, and software engineering, to monitor and record the main operating status of signal equipment, providing scientific basis for the electrical department to grasp the quality of equipment application and fault analysis. At the same time, the system also has the function of data logic judgment. When the working condition of the signal equipment deviates from the predetermined limit or abnormal occurs, it will alarm in a timely manner to avoid affecting the safety and punctual operation of the train due to equipment failure or illegal operation

The microcomputer monitoring system enables signal equipment to have self diagnosis function, thereby greatly improving the safety of the signal system. It can reflect the operating status of signal equipment 24/7 during operation, detect potential faults, eliminate hidden dangers, and use computer technology to logically judge, which is conducive to capturing instantaneous and intermittent faults. Through playback and reproduction, it is conducive to analyzing faults and distinguishing responsibilities. The microcomputer monitoring system can grasp the working status and trend of signal equipment, which is the technical basis for promoting signal equipment status maintenance and providing scientific basis for maintenance decision-making.

The transmission system functions and is technically safe according to the same process according to European standard EN50129. However, the use of untrusted transport systems limits the course of this functional approach. Therefore, the safety-related transmission system should be characterized by a functional specification including

an overall error model, and the safety integrity requirements specification should be formulated on the basis of a functional analysis of this error model. It is proposed in the functional integrity requirements that the design organization should provide six protective measures: check transmission identifier error, check data type error, check data value error, check the error of expired data or data not received within a predetermined time, check the data loss after a predefined delay, and ensure the independence of the security transmission function and the level of use of the untrusted transmission system. Meanwhile, six requirements should be fulfilled in the security integrity requirements: security protection should be applied to the generation of transmitted data; security response should be generated in the case of mis-operation, which is consistent with the security requirements of the receiver, the receiver applies an error checking mechanism and should be consistent with the receiver's security requirements; the use of the second clause in an untrusted transmission system should be functionally independent; the residual data error rate for each information exchange between sender and receiver within a safety-relevant transmission system should be less than a predetermined value. This ratio should be adapted to the safety integrity level (SIL) of each receiver.

Authenticity, integrity and accurate time of data should be ensured when communicating with each other between safety-related devices. In order to maintain the security required for communication between safety-related devices, the following requirements should be met: if the source of the transmission system is not uniquely specified, authenticity should be provided by adding a source indicator to user data; integrity should be provided by the user The security code is added to the data to provide, the security process can not only rely on the generated transmission code, but must be checked by the overall circuit as part of the untrusted transmission system; the timing of user data should be provided by adding time information to the user data., the time delay can be independent of the application [1–3]; it is necessary to set the order in which the safety process should check the information: the safety program of the safety-related device is functionally independent of the program used for the untrusted transmission system, if the two programs use the For the same coding structure, the parameters should also be different [4]; if the transmission quality falls below the pre-established transmission requirement specification level, an appropriate security response should be triggered. When safety and non-safety devices communicate with each other, safety-related and safety-independent information should have different structures, which is accomplished by applying secure coding to safety-related information [5]. This safety code shall protect the system to the required SIL from safety non-safety information to safety relevant information. The safety procedures of safety-related equipment should be functionally independent from the procedures used by untrusted transmission systems and safety-independent equipment [6].

In a complex network topology, the data transmission process will cause a series of errors, such as: packet loss, duplication, insertion, delay, timing errors, user data corruption and addressing errors [7]. From the perspective of the communication receiver, the following two communication errors may lead to dangerous situations:

1) data errors, such as: sending (receiving) address error, data type error, data value error;

2) timing errors, such as communication delay If it is too long, the sequence of sending and receiving data frames is inconsistent.

The goal of secure communication is to establish a protection mechanism to avoid the above errors during the transmission of security-related data, or when the above errors occur, the system can detect these errors in time and take necessary security measures [8].

In the existing computerized automatic inter-station blocking system, the real-time information is not checked in the secure communication layer, and only relies on the TCP/IP (Transmission Control Protocol/Internet Protocol) protocol of the untrusted transmission system to ensure that TCP is a connection-oriented end-to-end Reliable protocol and guarantees the order in which packets are delivered [9]. The sequence is guaranteed by the response sequence number, which tells the receiver the next packet the sender expects [10]. If the confirmation response is not received within the specified time, the packet needs to be resent. The reliable mechanism of TCP allows devices to handle lost, deleted and misread packets, and the pause mechanism allows devices to monitor lost packets and request retransmission [11].

The computer monitoring system is an important part of the modernization of railway equipment [12]. It integrates the latest modern technologies, such as sensors, fieldbus, computer network communication, database and software engineering, etc., to monitor and record the main operating status of the signal equipment, and provide the electric affairs department to master the use quality of the equipment and provide fault analysis. Scientific basis [13, 14]. At the same time, the system also has the function of data logic judgment. When the working condition of the signal equipment deviates from the predetermined limit or abnormality occurs, it will alarm in time to avoid equipment failure or illegal operation affecting the safe and punctual operation of the train [15]. The computer monitoring system enables the signal equipment to have a self-diagnosis function, thereby greatly improving the safety of the signal system [16]. When the signal equipment is running, it can reflect the operation status of the equipment all day long, and can find potential faults and eliminate hidden troubles. Moreover, it uses computer technology to make logical judgments, which is conducive to capturing instantaneous faults and intermittent faults, and reproducing them through playback. It is beneficial to analyze faults and distinguish responsibilities [17]. The types of detection objects can be roughly divided

into analog quantities and switch quantities. The analog quantities include: power screen voltage, track circuit voltage, switch operating current, cable insulation resistance and power supply-to-ground leakage current, etc. Switch quantities include: key relay status, Console button and identification lamp status, fuse status, filament status and turnout indicating gap status, etc. [18].

In order to improve the operation effect of the finite element multi-computer system, this paper proposes a distributed parallel algorithm for the finite element multi-computer system considering the performance evaluation of network security, and combines the experimental analysis to verify the algorithm effect to improve the operation reliability of the microcomputer system.

The innovation of this article lies in the study of using parallel computing technology to accelerate the calculation speed of DE for solving reactive power optimization problems, and implementing it on a microcomputer cluster platform. By improving the algorithm itself, the required population size is reduced, thereby further accelerating computation or using smaller clusters to reduce costs.

The contribution of this article is that the proposed distributed parallel algorithm has a certain promoting effect on the security improvement of finite element multi microcomputer systems, and also provides new references for related research.

2 Distributed Parallel Algorithms

2.1 Introduction of Differential Evolution Algorithms

The reason DE is named "differential evolution" is that the mutation operation of DE is not driven by a given random distribution function as in EP or ES, but by genetic differences between individuals randomly sampled from contemporary populations. For example, the form called DE/rand/1 shown in Equation (1):

$$\mathrm{DE}/rand/1 : u_{i,j}[k] + F(u_{r2,j}[k] - u_{r3,j}[k] \tag{1}$$

Among them, $r_1 \neq r_2 \neq r_3 \neq i \in \{1, 2, L, N\}$, that is, r1, r2 and r3 are integers randomly selected from the set $\{1, 2, \ldots, N\}$ that are not equal to each other and not equal to i; F is the proportional coefficient, which can be called the variation control coefficient.

According to the nomenclature of DE, $(u_{r1}[k])$ means to use the randomly selected individual as the basis of variation to form the increment of variation by the difference of a pair of randomly selected individuals.

We assume that there are only two control variables, then Equation (1) can be graphically illustrated by Figure 1 in a two-dimensional plane, and the ellipse in the figure represents the contour of the objective function.

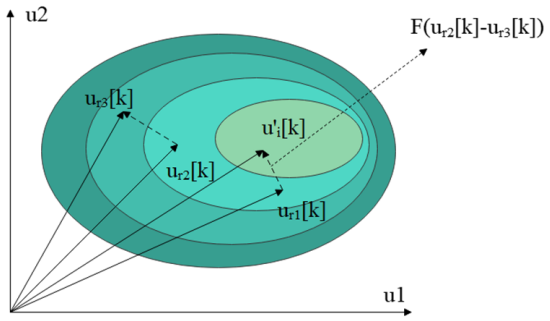

Figure 1: Schematic diagram of the variation of DE/rand/1

It is also possible to use the i-th individual $u_i[k]$ or the best contemporary individual $u_{best}[k]$ as the basis of variation instead of randomly selected individuals, and use the differences of more than one pair of individuals to form the variation increment, such as DE/current/1, DE/best/1, DE/rand/2, DE/current/2 and DE/best/2 as shown in Equations (2) - (6):

$$\mathrm{DE/current/1}: u_{i,j}[k] = u_{i,j}[k] + F(u_{r1,j}[k] - u_{r2,j}[k]) \tag{2}$$

$$\mathrm{DE/best/1}: u_{i,j}[k] = u_{best,j}[k] + F(u_{r1,j}[k] - u_{-2,j}[k]) \tag{3}$$

$$\mathrm{DE/rand/2}: u_{i,j}[k] = u_{i,j}[k] + F_1(u_{r2,j}[k] - u_{r3,j}[k]) + F_2(u_{r4,j}[k] - u_{rj}[k]) \tag{4}$$

$$\mathrm{DE/current/2}: u_{i,j}[k] = u_{i,j}[k] + F_1(u_{r1,j}[k] - u_{r2,j}[k]) + F_2(u_{r3,j}[k] - u_{r4,j}[k]) \tag{5}$$

$$\mathrm{DE/best/2}: u_{i,j}[k] = u_{best,j}[k] + F_1(u_{r1,j}[k] - u_{r2,j}[k]) + F_2(u_{r3,j}[k] - u_{r,j}[k]) \tag{6}$$

To speed up the search, DE also uses the hybridization operation. Discrete crossover was adopted in the early stage, mainly in two forms: "Binary Crossover" and "Exponential Crossover". Taking as an example, after introducing binary or exponential hybridization, two complete DE forms of DE/rand/1/bin and DE/rand/1/exp can be formed, as shown in Equations (7) and (8), respectively:

$$\mathrm{DE/rand/1/bin\ is}: u_{i,j}[k] = \begin{cases} u_{r1,j}[k] + F(u_{r2,j}[k] - u_{r3,j}[k], \\ if U_j(0,1) \leq \mathrm{CR}U_j = l_i \\ u_{i,j}[k], \quad otherwise \end{cases} \tag{7}$$

$$\mathrm{DE/rand/1/exp\ is}: \begin{cases} \mathrm{flag} = 1 \ \ if\ U_j(0,1) \leq \mathrm{CR}U_j = l_i \\ u_{r1,j}[k] = \begin{cases} u_{r1,j}[k] + F(u_{r2,j}[k] \\ -u_{r3,j}[k] if \mathrm{flag} = 1 \\ u_{i,j}[k], otherwise \end{cases} \end{cases} \tag{8}$$

Among them, $U_j(0,1)$ is a random number in the (0,1) interval, which is generated once for each control variable of individual i; $CR \in [0,1]$ is the given hybrid control coefficient; $l_i \in \{1,2,L,M\}$, which is generated only once for individual i.

Regarding the use of binary hybridization or exponential hybridization, the article points out that there is no significant difference in the effectiveness of the two hybridization forms in most cases, but the ability of binary hybridization to search the corners of hypercubes is stronger. Figure 2 graphically depicts a binary cross, in which a total of 8 control variables are assumed.

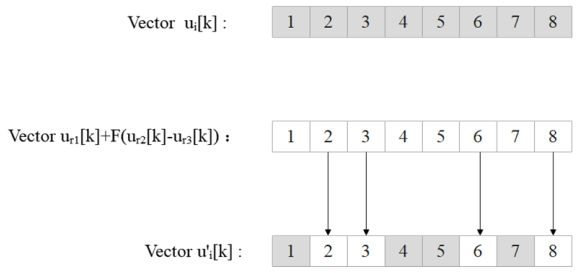

Figure 2: Schematic diagram of binary hybridization

The selection operation usually used by DE is "Binary Tournament Selection", which can also be more vividly called "one-to-one father-son competition", that is, comparing each child individual $u\mathbf{Mei}[k]$ with its parent individual $u_i[k]$, the one with higher fitness wins and enters the next generation, which becomes $u_i[k+1]$, as shown in Equation (9):

$$u_i[k+1] = \begin{cases} u_{i,i}[k], & \text{if} f'_i(k) \geq f_i(k) \\ u_i[k], & \text{if} f_i(k) \geq f'_i(k) \end{cases} \tag{9}$$

In Equation (9), the greater than or equal sign is used instead of the greater than sign, which helps to cope with the situation that the shape of the search space contains a platform part, so that the search process can "climb" over the platform.

2.2 Optimization Mechanism and Parameter Setting Analysis of Differential Evolution Algorithm

The advantages of DE's mutation operation are analyzed in detail, and it is considered that although it is very simple, it meets three conditions for becoming an excellent mutation operation:

Condition 1: The generated variation increments must conform to a random distribution centered at 0.

Condition 2: The magnitude of variation of each control variable should be dynamically changed to suit the shape of the search space. This condition actually contains the law that the author summarized for EP in the previous chapter, and it is more demanding.

Condition 3: The variation of each control variable should be correlated with each other to ensure rotational Invariance.

For Condition 1, if the center is not 0, the subgroup will have a fixed cumulative drift relative to the parent group, thus weakening the global search ability of the algorithm. The Gaussian distribution, the Cauchy distribution, or the more general Levy distribution used by EP and ES mentioned in the previous chapter all satisfy this condition. In Equation (1), since the selection of r1 and r2 is random, the probability of $U_{r1,j}[k] - u_{r2,j}[k]$ and $U_{r2,j}[k] - u_{r1,j}[k]$ appearing is the same, so the $F(U_{r1,j}[k] - u_{r2,j}[k])$ term also conforms to the random distribution centered on 0.

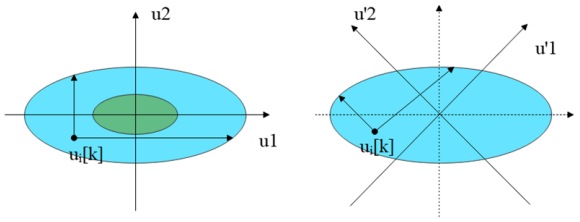

Figure 3: Illustration of Condition 2 and Condition 3

For Conditions 2 and 3, it can be understood with reference to Figure 3, which assumes that there are only two control variables, and the shape of the contour of the objective function is an ellipse. The left picture shows the case where the directions of the major and minor axes of the ellipse are the same as the coordinate axes. From this, it can be seen that at the same time, the effective variation range of different control variables is different, and with the progress of the optimization process, the effective variation range of each control variable is generally smaller and smaller, so as to adapt to the situation that the contour of the objective function changes from a large ellipse to a small ellipse.

Figure 4 shows the distribution of a population with four individuals (left panel) and its corresponding distribution of difference vectors (right panel, scale factor F=1). It can be seen that the distribution of the difference vector is a symmetrical distribution centered at 0, and its shape changes dynamically with the change of the population distribution. With the assistance of the selection operation, the shape of the search space can be gradually adapted, and only a scalar parameter F is needed to adjust the variation amplitude in each direction. Moreover, since the coordinate rotation will not change the relative position between individuals and the relative position of the entire population in the search space, it will not affect the performance of DE.

However, the aforementioned discrete hybridization would destroy the rotational independence. Figure 5

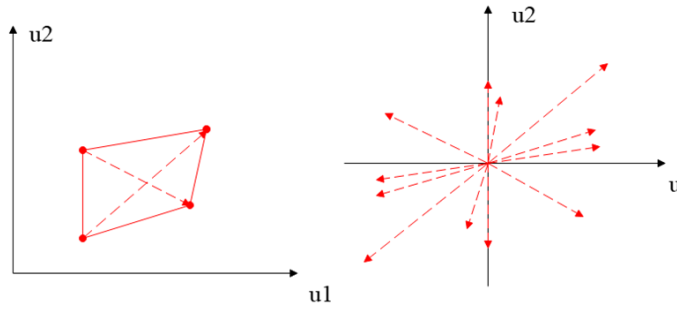

Figure 4: Schematic diagram of difference vector distribution

shows the hybridization of two individuals u and u in two dimensions. The position of the discrete hybridization result ($uXuu'$) will change with the rotation of the coordinate axis. However, if continuous linear hybridization is used like some ES methods, that is, the result of hybridization is on the connecting line of u and u, it will not be affected by the rotation of the coordinate axis.

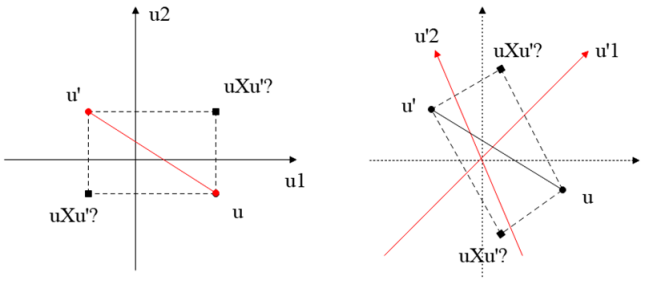

Figure 5: Schematic diagram of discrete hybridization and linear hybridization

Therefore, DE is more inclined to use linear hybridization, and the hybridization and mutation are directly combined together to form a concise and complete DE form, such as DE/current-to-rand/1 and DE shown in Equations (10) and (11). /current-to-best/1, where DE/current-to-rand/1 is the preferred form of DE recommended by K.V.Price.

DE/*current - to - rand*/1:

$$u'_{i,j}[k] = u_{i,j}[k] + K(u_{r1,j} - u_{i,j}[k]) + F(u_{r2,j}[k] - u_{r3,j}[k]) \tag{10}$$

DE/*current - to - best*/1:

$$u'_{i,j}[k] = u_{i,j}[k] + K(u_{best,j} - u_{i,j}[k]) + F(u_{r1,j}[k] - u_{r2,j}[k]) \tag{11}$$

Among them, K is called the hybridization control coefficient; u_{best} is the best individual that has appeared until the current generation, which may be called "the best individual in history".

The optimization mechanism of DE/current-to-best/1 can be illustrated by Figure 6: The function of the

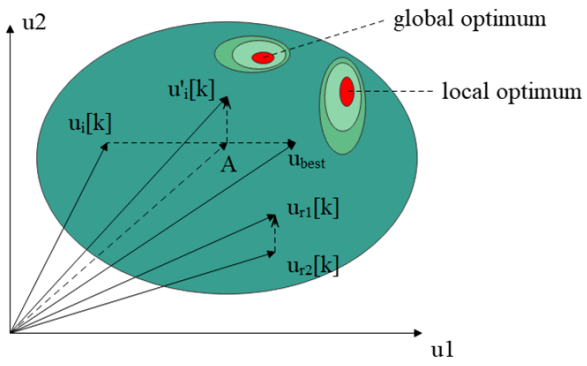

Figure 6: Schematic diagram of the mechanism of DE/current-to-best/1

$K(u_{best,j} - u_{i,j}[k])$ term is to "accelerate" each individual u_{best} (a search point) in the contemporary group towards u_{best} to a point A halfway (the case of $0 \leq K \leq 1$). The function of the $F(u_{r2,j}[k] - u_{r3,j}[k])$ term is to impose a perturbation on the search point at A, and the direction and intensity of the perturbation are determined by the difference between F and the two individuals u_{r1} and u_{r2} randomly selected from the current population, and finally a new individual u_i is obtained.

The flow chart of reactive power optimization based on DE/current-to-best/1 is shown in Figure 7.

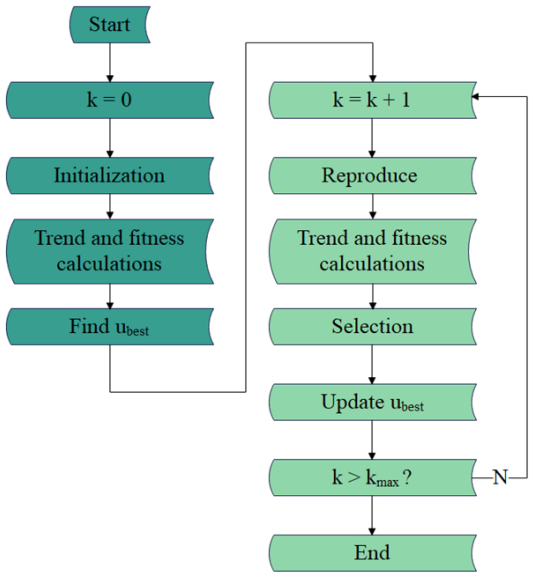

Figure 7: Flowchart of reactive power optimization based on DE/current-to-best/1

In the 0-th generation, the initialization is performed first to generate an initial group containing N individuals, then the power flow and fitness are calculated for each individual, and the best individual is found, which is the initial u_{best} .

In the k-th generation ($1 = k = k_{\max}$), firstly, the existing group (parent group) is reproduced according to Equation (11) to generate a sub-group, then the trend and fitness are calculated for each individual in the subgroup. Then, the individuals with the same numbers in the subgroup and the parent group conduct "one-to-one father-son competition", and the winner enters the next generation of the parent group, and the best contemporary individual $u_{best}[k]$ is found. If $u_{best}[k]$ is better than the historical best individual u_{best}, it is replaced by u_{best}.

2.3 Complementarity of Differential Evolution and Evolutionary Programming Algorithms

Regarding the reason why DE is prone to fall into premature convergence, it is believed that because DE adopts a relatively "greedy" selection operation of "one-to-one father-son competition", which leads to a rapid decline in population diversity and premature convergence. It adopts the selection operation of "one-to-one father-son competition", or adopts the relatively less "greedy" q-stakes selection like EP, or adopts the "greedier" deterministic selection operation like ES, and the performance shown by DE are not much different. It can be seen that the selection operation of "one-to-one father-son competition" is not the main reason.

The main reason is that there is no truly random mutation operation like in EP in the reproduction of DE, and the article also holds this view. For the convenience of explanation, the reproduction formulas of DE and EP are rewritten as follows:

DE/current-to-best/1 is:

$$u'_{i,j}[k] = u_{i,j}[k] + K(u_{best,j} - u_{i,j}[k]) + F(u_{r1,j}[k] - u_{r2,j}[k]) \quad (12)$$

$$EP : u_{i,j}[k] = u_{i,j}[k] + \rho_{i,j}[k]\dot{N}_{i,j}(0,1)[k] \quad (13)$$

Due to the mutation operation of DE, the last term in Equation (12), it consists of the difference between two individuals randomly selected from the current population. Therefore, the variation direction of each individual is limited. Because of the population size, there are (N-1) (N-2) mutation directions in total. The limited variation direction may affect the global search ability of DE in solving complex problems, and the population will be rapidly homogenized and fall into premature maturity. The expansion of the population size can not only expand the distribution of sampling, but also increase the variation direction of each individual, which is obviously beneficial to preventing precocious puberty, but it will increase the calculation time.

2.4 Design of a Hybrid Algorithm of Differential Evolution and Evolutionary Programming

For reactive power optimization, DE is a relatively excellent new evolutionary algorithm that deserves further research and application. However, it was also found that DE requires a relatively large population size to avoid premature convergence. This will result in a long calculation time, which cannot meet the needs of online reactive power optimization. By adopting parallel DE and appropriately sized clusters, online reactive power optimization of the power system can be effectively achieved; However, it is still necessary to find ways to reduce the required group size for DE to further accelerate computation or use smaller clusters to reduce costs.

A simple and effective hybrid solution of DE and EP was found and named DEEP. The scheme adopts the mechanism of main group plus auxiliary group. It refers to the group originally used in the evolution of DE as the main group, and the group size is N. Before reproduction in each generation, based on the first L (1=L=N) individuals in the main population, an auxiliary population of size L is generated according to an EP-type random mutation operation. The situation at the k-th generation is shown in Figure 8.

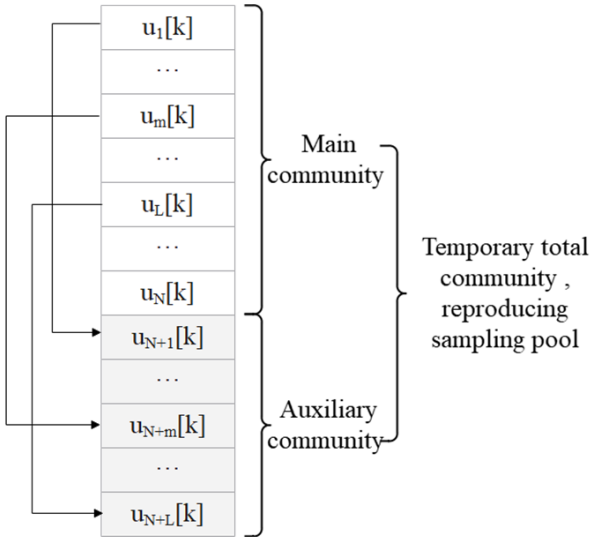

Figure 8: Schematic diagram of the generation of helper populations in DEPP (k-th generation)

After trial and error, it is found that the simple mutation operation shown in Equation (14) works well:

$$u_{N+m,j}[k] = u_{m,j} + U_{m,j}(0,1)\frac{f_{best} - f_m[k]}{f_{best} - f_{worst}}(u_j^{max} - u_j^{min}) \quad (14)$$

Among them, 1=m=L, 1=j=M, and M is the number of control variables. $U_{m,j}(0,1)$ generates a uniformly distributed random number located in the (0,1) interval each time; $f_m[k]$ is the fitness value of the m-th individual $u_m[k]$; f_{best} is the fitness value of the best individual u_{best} in history. f_{worst} is the fitness value of the worst individual u_{worst} in history; $(f_{best} - f_m[k])/(f_{best} - f_{worst})$ term provides an adaptive adjustment mechanism to the variation range of u_m, $[k]$, and its value gradually changes from large to small with the progress of the evolution process.

In each generation, the worse individuals have a larger variation range, and the better individuals have a smaller variation range. The $(u_j^{max} - u_j^{min})$ term is used to limit the variation range of the j-th control variable of each individual, and the value after guiding the variation should fall within $[u_j^{min}, u_j^{max}]$ as much as possible.

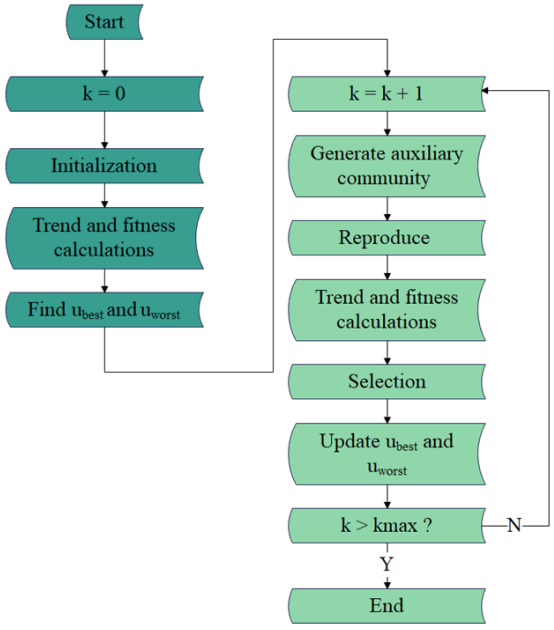

Figure 9: Flowchart of reactive power optimization based on DEEP

Since the hybrid scheme is very simple, the calculation process of DEEP differs little from that of DE. Figure 9 is a flow chart of DEEP-based reactive power optimization.

In the 0-th generation, initialization is performed first to generate an initial population containing N individuals. Then, the trend and fitness are calculated for each individual. Then, the best individual u_{best} and the worst individual u_{worst} are found, that is, the initial historical best individual and the historical worst individual. The initial population is used as the main parent population in generation 1.

In the k-th generation $(1 = k = k_{\max}())$, based on the first L individuals in the main parent group, an auxiliary parent group of size L is generated according to formula (14). Then, according to the above description, a subgroup of size N is generated based on the temporary general parent group of size N+L synthesized by the main and auxiliary parent groups. Then, the power flow and fitness are calculated for each individual in the subgroup. Then, the individuals with the same number in the subgroup and the main parent group conduct "one-to-one father-son competition", and the winner enters the main parent group of the next generation. The contemporary best individual $u_{best}[k]$ and the contemporary worst individual $u_{worst}[k]$ are also found from the winners, if $u_{best}[k]$ is better than the historical best individual u_{best}, it is replaced by u_{best}. If a new parameter appears in the $u_{worst}[k]$ ratio history DEEP, that is, the size of the auxiliary population L, it needs to be determined through experiments. More generally, the determination of L may be replaced by the determination of the ratio of L to N, L/N.

DE and EP can be described as follows: DE is better at mining existing genetic information in the population, but not at introducing new genetic information, that is, exploring new fields in the search space, Therefore, the convergence speed is fast but it is easy to fall into premature puberty; EP, on the other hand, constantly introduces new genetic information without fully utilizing it, making it less likely to fall into early puberty but with slow convergence. It can be clearly seen that DE and EP have good complementarity and can be combined to construct a hybrid algorithm that leverages strengths and avoids weaknesses

2.5 Grid Partitioning Based on Reactive Voltage Sensitivity and Clustering Technology

In order to realize grid partitioning, the electrical distance between nodes is firstly defined based on the reactive power and voltage sensitivity between nodes. The definition is shown in Equation (15):

$$d_{ij} = -\log(a_{ij}a_{ji} \tag{15}$$

$$a_{ij} = \frac{\partial V_i}{\partial Q_i} / \frac{\partial V_j}{\partial Q_j} \tag{16}$$

Among them, dij represents the electrical between nodes i and j; Vi and Vj are the voltages at nodes i and j, respectively; Qj is the reactive power injection at node j.

Commonly used interval distances are defined as maximum distance, minimum distance, average distance and Ward distance, as shown in Equations (17) to (20), respectively.

The maximum distance is:

$$d_{max}(C_i, C_j) = max_{b\in C_i, b\in C_j} d(b, b') \tag{17}$$

The minimum distance is:

$$d_{min}(C_i, C_j) = min_{b\in C_i, b\in C_j} d(b, b') \tag{18}$$

The average distance is:

$$d_{avr}(C_i, C_j) = \frac{1}{k_i, k_j} \sum_{b\in C_i} \sum_{b\in C_j} d(b, b') \tag{19}$$

Ward distance is:

$$d_{ward}(C_i, C_j) = \frac{k_i k_j}{k_i + k_j} d(o_i, o_j) \tag{20}$$

Among them, C_i and C_j represent the partitions numbered i and j; $d()$ represents the distance; b represents the node; k_i and k_j represent the number of nodes in partitions C_i and C_j ; o_i and o_j represent the "central

nodes" of partitions and . The central node of a partition is defined as the node with the smallest sum of squared distances from all other nodes in the same region.

The clustering validity index (CVI) is an index used to evaluate the quality of the clustering scheme (here, the partition scheme), and there are many definitions of CVI. Among them, the four definitions of Global Silhouette Index(GSI), Davis-Bouldin Index(DBI), Dunn's Index(DI) and C Index(CI) have clear and relatively simple physical meanings, which are introduced as follows.

2.5.1 Global Silhouette Index (GSI)

$$GSI = \frac{1}{L}\sum_{j=1}^{L} S(C_j)$$

$$S(C_j) = \frac{1}{K_j}\sum_{i=1}^{k_j} S(b_i)$$

$$S(b_i) = \frac{y(b_i)-x(b_i)}{\max\{x(b_i),y(b_i)\}} \quad (21)$$

$$x(b_i) = \frac{1}{KJ}\sum_{b_i,b\in c_j} d(b_i,b_l)$$

$$y(b_i) = min_{j\neq j\in\{1,2,L,L_j\}}(\frac{1}{k_j}\sum_{b_i\in C_j}^{b_i\in C_j} d(b_i,b_j))$$

Among them, $x_(b_i)$ represents the average distance between the i-th node b_i in the partition C_j and other nodes in the same region. $S(b_i)$ is called the "Silhouette Width" of , and is used to represent the "Confidence Index" that b_i belongs to $c_j\dot{S}(b_i)$. is close to 1, indicating that b_i has been assigned to the correct partition. $S(b_i)$ is close to 0, indicating that b_i can also be classified into adjacent partitions; When $S(b_i)$ is close to -1, it means that b_i is classified into the wrong partition. L is the number of partitions, and the GSI indicator is the average Silhouette width of the entire partition scheme. The larger the GSI, the better the partitioning scheme.

2.5.2 Davis-Bouldin Index (DBI)

$$DBI = \frac{1}{L}\sum_{i=1}^{L} min_{j\neq i\in\{1,2,L,L\}} D_{i,j}$$

$$D_{ij} = \frac{y(C_i,C_j)}{x(C_i)+x(C_j)} \quad (22)$$

$$x(C_i) = \frac{1}{k_i}\sum_{b_l\in C_i} d(b_l,o_i)$$

Among them, $x(C_i)$ represents the average distance between all nodes in partition C_i and the central node of the partition; $y(C_i,C_j)$ represents the distance between the central nodes of partitions C_i and C_j. The larger the DBI, the more compact the nodes in the same partition, and the more scattered the centers of different partitions, that is, the better the clustering results.

2.5.3 Dunni Index (DI)

Among them, D_{min} represents the minimum distance between two nodes belonging to different partitions, and D_{max} represents the maximum distance between two nodes belonging to the same partition. The larger the DI, the better the clustering result.

$$DI = D_{min}/D_{max}$$

$$D_{min} = min_{b_l\in C_c,b_{12}\in C_j,i\neq j\in\{1,2,L,L_j\}} d(b_{l1},b_{l2} \quad (23)$$

$$D_{max} = max_{b_l,h_2\in C_i,i\in\{1,2,\perp,L\}} d(b_{l1},b_{l2})$$

2.5.4 C Index (CI)

Among them, S represents the sum of the distances between all nodes in the same area of the L partitions; there are N_d such distances in total, and S_{min} and S_{max} respectively represent the sum of the N_d minimum and maximum distances among the distances between all N_b nodes in the entire power grid $N_b * (N_b - 1)/2$total. Likewise, the larger the CI, the better the clustering result.

$$\min F = \sum_{j=1}^{L}\sum_{b_i\in C_j} d^2(b_i,o_j) \quad (24)$$

Among them, the meaning of each symbol is the same as the previous one, which is reiterated as follows: L is the number of partitions, b_i is the i-th node in partition c_j, o_j, is the central node of partition C_j, and $d(b_j,o_j)$ represents the electrical distance between b_i and o_j.

3 Distributed Parallel Algorithm for Finite Element Multi-computer System Considering Network Security Performance Evaluation

The function of the microcomputer measurement and control protection is to collect the power information of the line and monitor the running status of the system in real time. When a fault is detected, it immediately performs a protection operation to trip the circuit breaker, or quickly uploads the fault information to the upper computer to achieve fault location, and executes the control commands sent by the upper computer. The system block diagram of the microcomputer measurement and control protection device designed in this paper is shown in Figure 10. In order to verify the correctness of the distributed parallel algorithm, input a 100V, 50Hz square wave to analyze the distributed parallel algorithm, and use the DA module to output the detection results of the fundamental wave instantaneous value. At the same time, the FFT function of the oscilloscope is used to detect the effective value of the fundamental wave of the input signal and compare it with the calculation result of the distributed parallel algorithm, as shown in Figure 11.

Figure 11(a) shows the waveform of the instantaneous value of the fundamental wave calculated by the input square wave and the distributed parallel algorithm. The

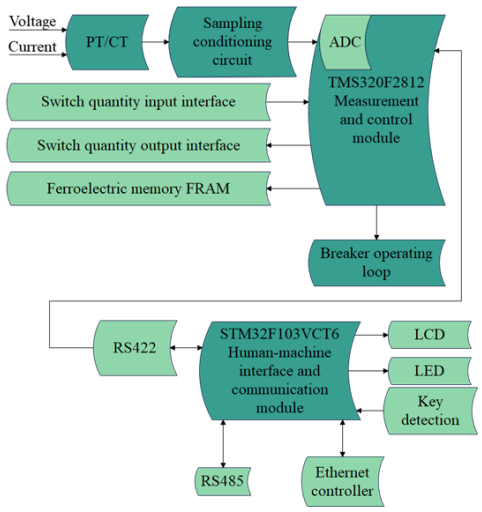

Figure 10: System structure of microcomputer protection device

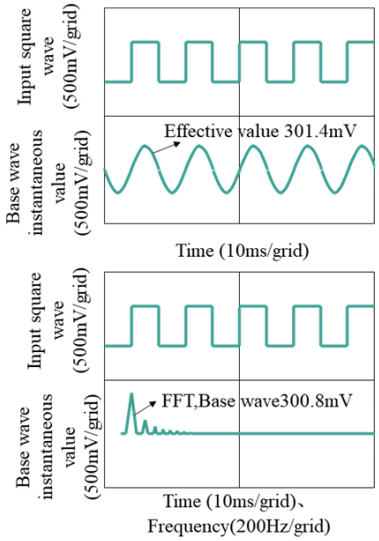

Figure 11: Experimental results of distributed parallel algorithm for detecting square waves

oscilloscope shows that the effective value of the fundamental wave is 301.4mV (attenuated by 300 times). (b) is the result of square wave analysis using the oscilloscope FFT function, and the effective value of the fundamental wave is 300.8V. The two are approximately equal within the allowable error range, indicating that the distributed parallel algorithm correctly detects the fundamental wave of the input signal.

Sinusoidal signals with a voltage of 100V and frequencies of 50Hz, 49.5Hz, and 50.5Hz are input, and the DA module is used to output the fundamental RMS calculation result of the distributed parallel algorithm. The experimental waveform is shown in Figure 12. When using the further method, the system poles are outside the unit circle. Obviously, the RMS calculation result of the distributed parallel algorithm gradually diverges from 100V at this time, and finally is limited because it exceeds the range of DA representation. During simulation, the limit is limited because it exceeds the fixed-point representation range of Q15, and the limit value here is smaller than that during simulation. The divergence mode is different at different frequencies, but the overall increase is gradually increased, and the distributed parallel algorithm is unstable.

Table 1: The security improvement of the distributed algorithm for the finite element multi-computer system

No.	Safety	No	Safety	No	Safety
1	91.117	11	89.725	21	86.174
2	87.075	12	88.076	22	89.049
3	87.538	13	90.386	23	85.512
4	84.366	14	90.339	24	91.662
5	88.596	15	89.399	25	89.533
6	91.908	16	85.001	26	88.239
7	88.716	17	88.991	27	87.546
8	87.759	18	85.247	28	89.188
9	86.625	19	91.337	29	87.604
10	91.994	20	86.513	30	90.129

Through the above research, the effectiveness of the distributed parallel algorithm proposed in this paper is verified. On this basis, the effect of the distributed algorithm in the security improvement of the finite element multi-computer system is carried out, and 30 sets of data are tested, and the results shown in Table 1 below are obtained. To further verify the effectiveness of the model proposed in this paper, the same experimental method was used for simulation. The model was compared with the method proposed in Reference [10], and their algorithm performance and network security were compared. The comparison results are shown in Table 2 and Table 3 below

It can be seen from the above research that the distributed parallel algorithm proposed in this paper has a certain promotion effect on the security improvement of

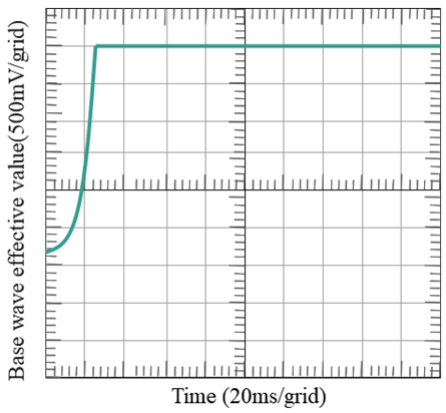

(a) 20ms/grid

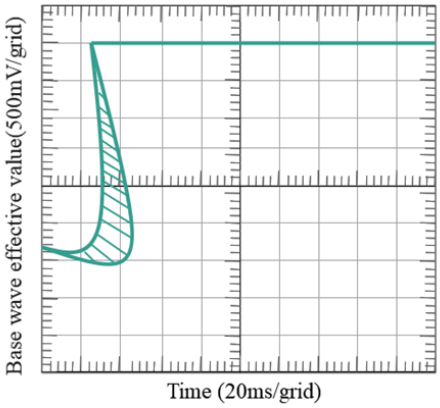

(b) 49.6Hz

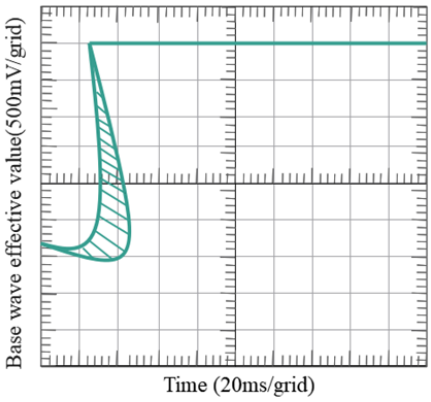

(c) 50Hz

Figure 12: The experimental results of the distributed parallel algorithm to calculate the fundamental wave RMS at different frequencies

Table 2: Comparison of Algorithm Performance

	The Proposed Method	**Reference [10]**
1	84.72	79.41
2	85.67	79.27
3	83.94	79.04
4	85.61	81.63
5	83.85	82.20
6	84.47	79.24
7	81.70	78.39
8	88.99	78.38
9	83.54	82.19
10	81.98	75.07
11	86.18	75.56
12	84.24	82.99
13	82.23	81.18
14	82.88	81.10
15	83.85	81.59

Table 3: Network security comparison

	The Proposed Method	**Reference [10]**
1	93.93	81.68
2	93.45	80.96
3	91.49	78.00
4	87.56	76.85
5	93.04	80.57
6	90.16	82.07
7	87.24	75.86
8	91.08	77.80
9	92.32	78.74
10	92.09	75.58
11	90.50	79.60
12	93.58	78.60
13	87.41	81.00
14	91.36	78.17
15	91.63	82.58

the finite element multi-computer system.

4 Conclusions

In order to test the safety communication program of the computerized automatic inter-station blocking system, a computerized automatic inter-station blocking system safety communication simulation subsystem is designed to analyze the inter-station communication messages and simulate the inter-station communication fault setting. The microcomputer monitoring system can grasp the working status and changing trend of the signal equipment, which is the technical basis for the implementation of the status repair of the signal equipment, and provides a scientific basis for the maintenance decision. The computer monitoring system uses computers and information acquisition machines to detect various signal devices in real time. This paper proposes a distributed parallel algorithm for finite element multi-computer system considering network security performance evaluation, and combines the experimental analysis to verify the algorithm effect. The experimental analysis shows that the distributed parallel algorithm proposed in this paper is effective, and it verifies that the distributed parallel algorithm proposed in this paper has a certain promotion effect on the security improvement of the finite element multi-computer system.

The subsequent research work is to combine DE with interior point method, complement each other's strengths and weaknesses, and construct a universal and effective hybrid algorithm suitable for solving reactive power optimization problems.

References

[1] A. Al-Halafi and Shihada B. Uhd, "video transmission over bidirectional underwater wireless optical communication," *IEEE Photonics Journal*, vol. 10, no. 2, pp. 1–14, 2018.

[2] Nourah Almrezeq, Mamoona Humayun, Madallah Alruwaili, Saad Alanazi, and NZ Jhanjhi, "Cyber security attacks and challenges in saudi arabia during covid-19," *International Journal of Computer Science & Network Security*, vol. 23, no. 10, pp. 179–187, 2023.

[3] Neda Azizi and Omid Haass. "Cybersecurity issues and challenges,". in *Handbook of Research on Cybersecurity Issues and Challenges for Business and FinTech Applications*, pp. 21–48. IGI Global, 2023.

[4] J. Barowski, M. Zimmermanns, and I. Rolfes, "Millimeter-wave characterization of dielectric materials using calibrated fmcw transceivers," *IEEE Transactions on Microwave Theory and Techniques*, vol. 66, no. 8, pp. 3683–3689, 2018.

[5] B. Behroozpour, "Sandborn p a m, wu m c, et al. lidar system architectures and circuits," *IEEE Communications Magazine*, vol. 55, no. 10, pp. 135–142, 2017.

[6] Q. Y. Cheng, X. L. Zhao, Y. X. Weng, et al., "Fully sustainable, nanoparticle-free, fluorine-free, and robust superhydrophobic cotton fabric fabricated via an eco-friendly method for efficient oil/water separation," *ACS Sustainable Chemistry & Engineering*, vol. 7, no. 18, pp. 15696–15705, 2019.

[7] Y. Jiang, S. Karpf, and B. Jalali, "Time-stretch lidar as a spectrally scanned time-of-flight ranging camera," *Nature photonics*, vol. 14, no. 1, pp. 14–18, 2020.

[8] H. C. Kumawat and A. B. Raj, "Extraction of doppler signature of micro-to-macro rotations/motions using continuous wave radar-assisted measurement system," *IET Science, Measurement & Technology*, vol. 14, no. 7, pp. 772–785, 2020.

[9] N. Maring, P. Farrera, K. Kutluer, et al., "Photonic quantum state transfer between a cold atomic gas and a crystal," *Nature*, vol. 551, no. 7681, pp. 485–488, 2017.

[10] Z. Meng, J. Li, C. Yin, et al., "Dual-band dechirping lfmcw radar receiver with high image rejection using microwave photonic i/q mixer," *Optics express*, vol. 25, no. 18, pp. 22055–22065, 2017.

[11] H. Mohapatra and Rath A. K. Detection and, "and avoidance of water loss through municipality taps in india by using smart taps and ict," *IET wireless sensor systems*, vol. 9, no. 6, pp. 447–457, 2019.

[12] Z. Sabouri, A. Akbari, H. A. Hosseini, et al., "Eco-friendly biosynthesis of nickel oxide nanoparticles mediated by okra plant extract and investigation of their photocatalytic, magnetic, cytotoxicity, and antibacterial properties," *Journal of Cluster Science*, vol. 30, no. 6, pp. 1425–1434, 2019.

[13] A. Seri, G. Corrielli, D. Lago-Rivera, et al., "Laser-written integrated platform for quantum storage of heralded single photons," *Optica*, vol. 5, no. 8, pp. 934–941, 2018.

[14] Imdad Ali Shah, NZ Jhanjhi, and Areeba Laraib. "Cybersecurity and blockchain usage in contemporary business,". in *Handbook of Research on Cybersecurity Issues and Challenges for Business and FinTech Applications*, pp. 49–64. IGI Global, 2023.

[15] L. J. Xu, X. Lin, Q. He, et al., "Highly efficient eco-friendly x-ray scintillators based on an organic manganese halide," *Nature communications*, vol. 11, no. 1, pp. 1–7, 2020.

[16] F. Zhang, Q. Guo, and S. Pan, "Photonics-based real-time ultra-high-range-resolution radar with broadband signal generation and processing," *Scientific reports*, vol. 7, no. 1, pp. 1–8, 2017.

[17] T. Zhong and P. Goldner, "Emerging rare-earth doped material platforms for quantum nanophotonics," *Nanophotonics*, vol. 8, no. 11, pp. 2003–2015, 2019.

[18] T. Zhong, J. M. Kindem, J. G. Bartholomew, et al., "Nanophotonic rare-earth quantum memory with

optically controlled retrieval," *Science*, vol. 357, no. 6358, pp. 1392–1395, 2017.

Biography

Yi Li was born in Henan, China, in 1980. From 1999 to 2003, she studied in Zhengzhou University of Light Industry and received her bachelor's degree in 2003. From 2006 to 2009, she studied in Huazhong University of Science and Technology and received her Master's degree. Currently, she worked in Henan Judicial Police Vocational College, Zhengzhou. Her research fields include computer education, Big data visualization and application and digital graphic image processing.